MINERALOGY, GEOCHEMISTRY AND GENESIS OF SMECTITE IN PLIOCENE VOLCANICLASTIC ROCKS OF THE DOĞANBEY FORMATION, BEYŞEHİR BASIN, KONYA, TURKEY

SELAHATTİN KADİR*

Eskişehir Osmangazi University, Department of Geological Engineering, TR-26480 Eskişehir, Turkey

Abstract—Pliocene volcaniclastic lacustrine rocks of the Doğanbey formation in the Beyşehir region (central Anatolia) are composed of organic-matter-bearing claystone, clastic units and dolomite interbeds, suggesting an anaerobic, shallow swampy, lacustrine depositional environment. The depositional environment was subjected to periodic climatic change during which diagenesis occurred, and smectite, and locally palygorskite, were precipitated. Smectite flakes formed authigenically on feldspar and palygorskite fibers between dolomite rhombs and at the edges of smectite flakes. Increases in leaching of Na, K, Sr, Ba and Rb, increasing Al/Si ratios, and Fe with increasing degree of alteration reveal that hydration of volcaniclastic grains (feldspar, glass) by meteoric water − determined from O and H isotopic values − was the main cause of precipitation of beidellite and montmorillonite based on the tetrahedral charge/octahedral charge ratio, with average structural formulae of $(Si_{7.72}Al_{0.28})(Al_{3.20}Fe_{0.53}Mg_{0.25}Mn_{0.02}Ti_{0.04})(Ca_{0.11}Na_{0.09}K_{0.11})$, and $(Si_{7.88}Al_{0.13})(Al_{3.18}Fe_{0.53}Mg_{0.18}Mn_{0.02}Ti_{0.05})(Ca_{0.11}Na_{0.11}K_{0.09})$, respectively. Therefore, the Doğanbey-area smectite is presumed to have formed by chemical weathering and dissolution-precipitation from feldspar and glass during diagenesis; palygorskite formed by direct precipitation from Mg-rich solutions during dolomitization, and by transformation from smectite in an alkaline lacustrine environment.

Key Words—Geochemistry, Lacustrine Environment, Mineralogy, Smectite, Stable Isotopes, Turkey, Volcaniclastic Rocks.

INTRODUCTION

In nature, smectite develops either by *in situ* weathering, by diagenetic or hydrothermal alteration of volcanic-glass shards, feldspars, micas and ferromagnesian minerals (olivine, hornblende, augite) of pyroclastic rocks and lavas, by direct precipitation from solution (neoformation), or by detrital inheritance (Grim and Güven, 1978; Teale and Spears, 1986; Weaver, 1989; Christidis *et al.*, 1995; Yalçın and Gümüşer, 2000; Abdioğlu and Arslan, 2005). Primary minerals were dissolved by reaction with meteoric or hydrothermal fluids to form smectite.

High-pH waters favor precipitation of palygorskite, due to the increase in Mg and the decrease in Al during dolomitization (Weaver and Beck, 1977). The source of the fluid phase can be either meteoric (fresh), hydrothermal or sea water. Concentrated alkaline solutions for precipitation of smectite, palygorskite and dolomitization develop *via* evaporation of fresh or connate waters.

During late Miocene-Pliocene, volcanism produced widespread deposits of dacitic and andesitic ignimbrites and lacustrine sedimentary units in the Konya basin (central Anatolia) (Keller *et al.*, 1977; Temel *et al.*, 1998). These units were altered to smectite, halloysite, kaolinite, minamiite and jarosite in ignimbritic units, whereas carbonate and fluvial units are prevalent where sepiolite-palygorskite and smectite are found, respectively (Karakaş and Kadir, 1998; Kadir and Karakaş, 2002). Smectite and kaolinite occur in deposits with economic potential (Suludere *et al.*, 1986; Özgüner *et al.*, 1987). Alteration in the Konya volcano-sedimentary units has been attributed to hydrothermal activity (Suludere *et al.*, 1986; Temel *et al.*, 1995; and Çelik *et al.*, 1997), and to weathering (Kadir and Karakaş, 2002).

Although previous exploration has revealed smectite (bentonite) abundance in volcanic units, the occurrence of smectite in the volcaniclastic rocks of the Doğanbey region (Beyşehir) may indicate that the origin of smectite is still open to debate. In addition, no evidence for hydrothermal alteration − such as Fe- and S-bearing phases or concentration of smectite along faults − has been detected; moreover, smectite occurs in both the volcaniclastic rocks and the carbonate sediments (Figures 1−3). The objectives of the present study are to present the mineralogical, geochemical and stable-isotope characteristics of smectite, and to discuss the origin of smectite within the Pliocene lacustrine volcaniclastic environment.

METHODS

In order to identify the lateral and vertical distribution of smectite in the study area, six stratigraphic sections within the lacustrine volcaniclastic units of the

* E-mail address of corresponding author:
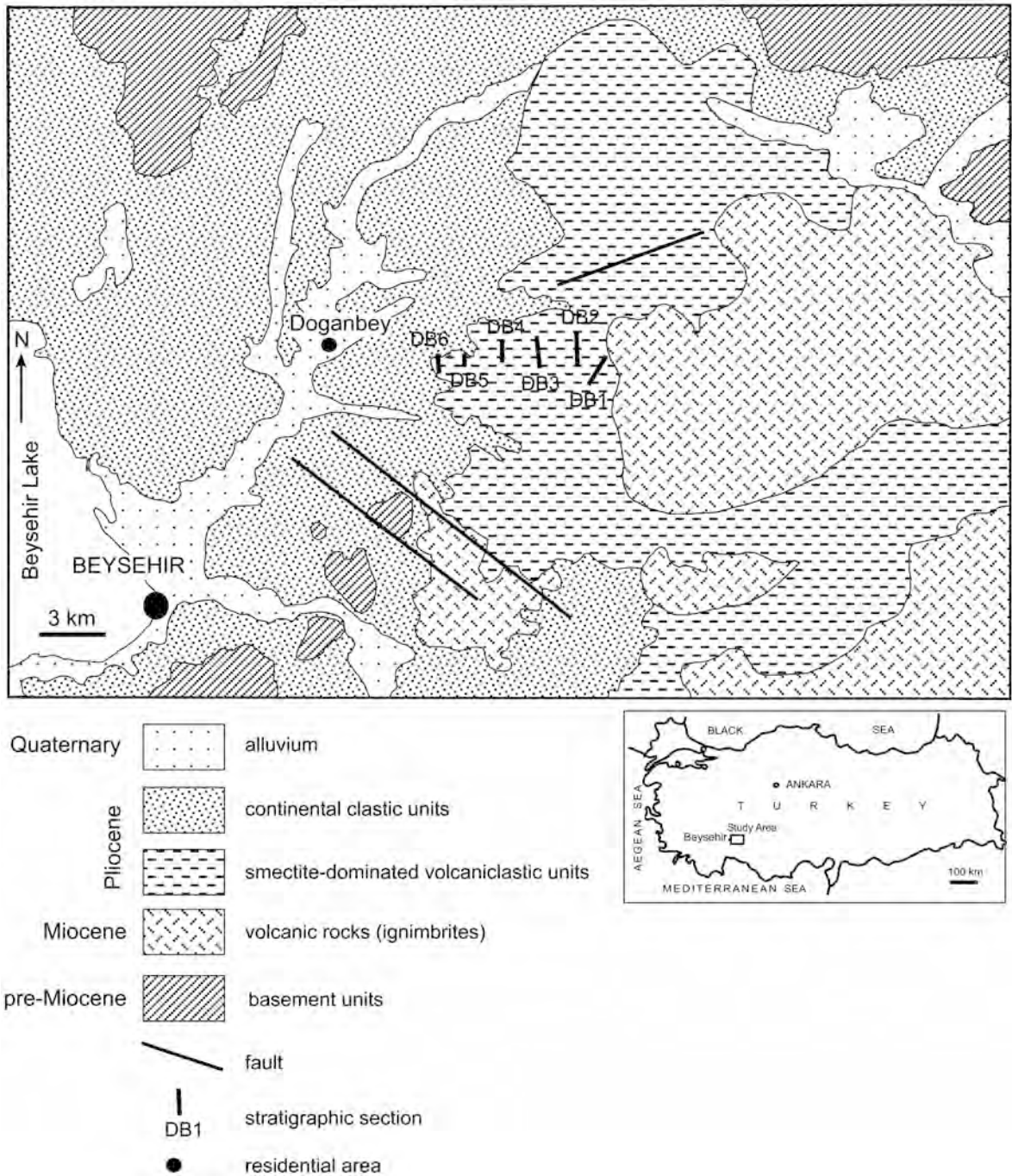skadir_ogu@yahoo.com

402

Figure 1. Geological map of the Doğanbey area (modified from Şenel, 2002).

Doğanbey formation were sampled (Figures 1–3). Sixty-five samples, representing the various facies, were analyzed for their mineralogical characteristics by polarized-light microscopy (Leitz Laborlux 11 Pol), powder X-ray diffractometry (XRD) (Rigaku-Geigerflex) and scanning electron microscopy (SEM-EDX) (JEOL JSM 84A-EDX). The XRD analyses were performed using CuKα radiation and a scanning speed of

1°2θ/min. Random powders of whole-rock samples were used to determine bulk mineralogy. Clay mineralogy was determined *via* separation of the clay fraction (<2 μm) by sedimentation after overnight dispersion in distilled water, followed by centrifugation of the suspension. The clay particles were dispersed by ultrasonic vibration for ~15 min. Five oriented specimens of the <2 μm fraction were prepared from each sample: air dried; ethylene
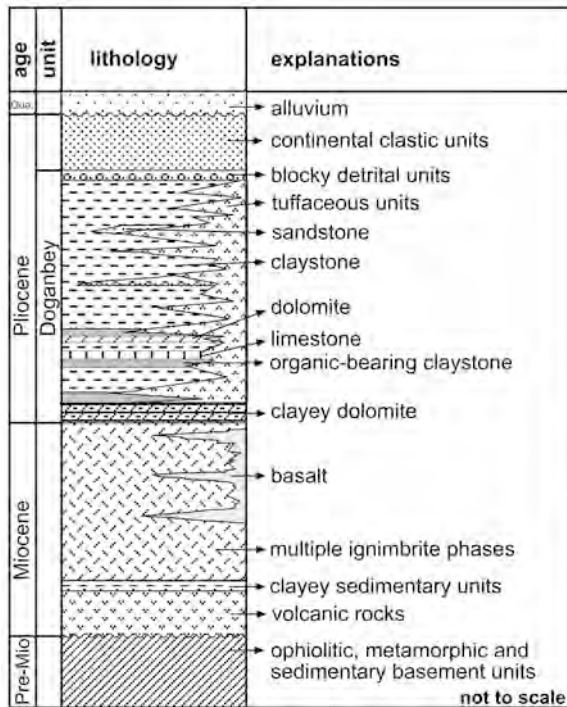
Figure 2. Simplified general stratigraphical section of the study area and surrounding area.

glycol solvated at 60ºC for 2 h; dimethylsulfoxide (DMSO) treatment; and thermally treated at 350ºC and 550ºC for 2 h. Semi-quantitative relative abundances of rock-forming minerals were obtained according to Brindley (1980), whereas the relative abundances of clay minerals were determined using their basal reflections and the intensity factors of Moore and Reynolds (1989). The presence of root imprints and organic material was determined by polished-section microscopy (Leitz MPV-SP). Representative clay-abundant bulk samples were prepared for SEM-EDX analysis by adhering the fresh, broken surface of each rock sample onto an aluminum sample holder using double-sided tape, and then coating with a thin film (350 Å) of gold using a Giko ion coater.

Chemical analyses of 22 whole-rock and five purified smectite fractions were carried out using inductively coupled plasma-atomic emission spectroscopy (ICP-AES) for major and trace elements at Acme Analytical Laboratories Ltd. (Canada). The detection limits for analyses were between 0.01 and 0.1 wt.% for major elements, and 0.1 and 5 ppm for trace elements.

Enrichments and depletions of elements have been estimated using the procedure of MacLean and Kranidiotis (1987). In these calculations, Al was assumed to be the most immobile element based upon calculated correlation coefficients with other elements. All samples were grouped on the basis of degree of alteration (average result from each group), and the

gains and losses of components were calculated by using a starting mass of 100 g of average fresh anhydrous sample. The equation used in calculations can be written for SiO_2 (MacLean and Kranidiotis, 1987) as:

$$SiO_2 = \frac{SiO_2 \text{ wt.\% altered rock}}{Al_2O_3 \text{ wt.\% altered rock}} \times Al_2O_3 \text{ wt.\% fresh rock}$$

Gains and losses of mass were determined by subtracting the calculated values from concentrations of components in least-altered samples using the formula above.

Smectite structural formulae were calculated from the chemical analyses of the 2 μm clay fractions with the largest smectite contents. Separation was undertaken following removal of free Fe oxides and organic matter using the sodium dithionite-citrate procedure and hydrogen peroxide (30%) treatment, respectively (Kunze and Dixon, 1986). The structural formulae of smectites were calculated based on $O_{20}(OH)_4$ assuming that the tetrahedral sites were filled with Si and Al to sum to 8. The remaining Al was assigned in octahedral sites. All Fe is ferric, and all Mg, Mn and Ti were assigned to octahedral sites. Calcium, Na and K were assigned to exchangeable interlayer cations.

Three smectite and palygorskite-bearing smectite samples were analyzed for stables isotopes of H and O by Activation Laboratories Ltd. (Actlabs) in Canada. The H isotopic analyses, carried out using conventional isotope ratio mass spectrometry, are reported in the familiar notation in per mil relative to the V-SMOW standard. The procedure described above was used to measure a δD value of −65‰ for the NSB-30 biotite standard. The O isotopic analyses were performed on a Finnigan MAT Delta, dual inlet, isotope ratio mass spectrometer, following the procedures of Clayton and Mayeda (1963). The data are reported in the standard delta notation as per mil deviations from V-SMOW. External reproducibility is ±0.19‰ (1σ) based on repeat analyses of internal white crystal standard (WCS). The NBS 28 value is 9.61 ±0.10‰ (1σ).

GEOLOGICAL SETTING

The basement of the study area comprises pre-Miocene metamorphic, ophiolitic and sedimentary units (Figures 1 and 2; Umut *et al.*, 1987; Zedef *et al.*, 1994) overlain unconformably by Upper Miocene−Pliocene volcanic rocks and lacustrine-fluvial sediments (Keller *et al.*, 1977). These units were termed the Upper Miocene Ulumuhsine and Pliocene Doğanbey formations by Temel *et al.* (1995). The study area includes the abundant and widespread smectite-bearing Doğanbey formation; the unit comprises lacustrine volcaniclastics which were transported from the east and south where volcanic units crop out.

Volcaniclastic units of the Doğanbey formation include claystone, limestone-dolomite-marl, sandstone-mudstone-conglomerate and tuff (Figures 2, 3). These units show lateral and vertical transitions.

Claystone

A yellowish-green, greenish-cream-colored, brown, variegated, medium hard, friable, plastic-type smectitic claystone unit contains prevalent amounts of root imprints and bears carbonate and/or silt-, sand- or pebble-type detrital sediment, and can be characterized as dolomitic claystone−clayey dolomite and silty-sandy-pebbly claystone. Moreover, in some places, the claystones bear relics of tuffaceous materials and glass shards, and thus are locally of tuffaceous claystone.

Claystone in which smectite and palygorskite are prevalent occur as friable organic-matter-bearing claystone facies (DB1-15, DB1-16). The silty claystone has a
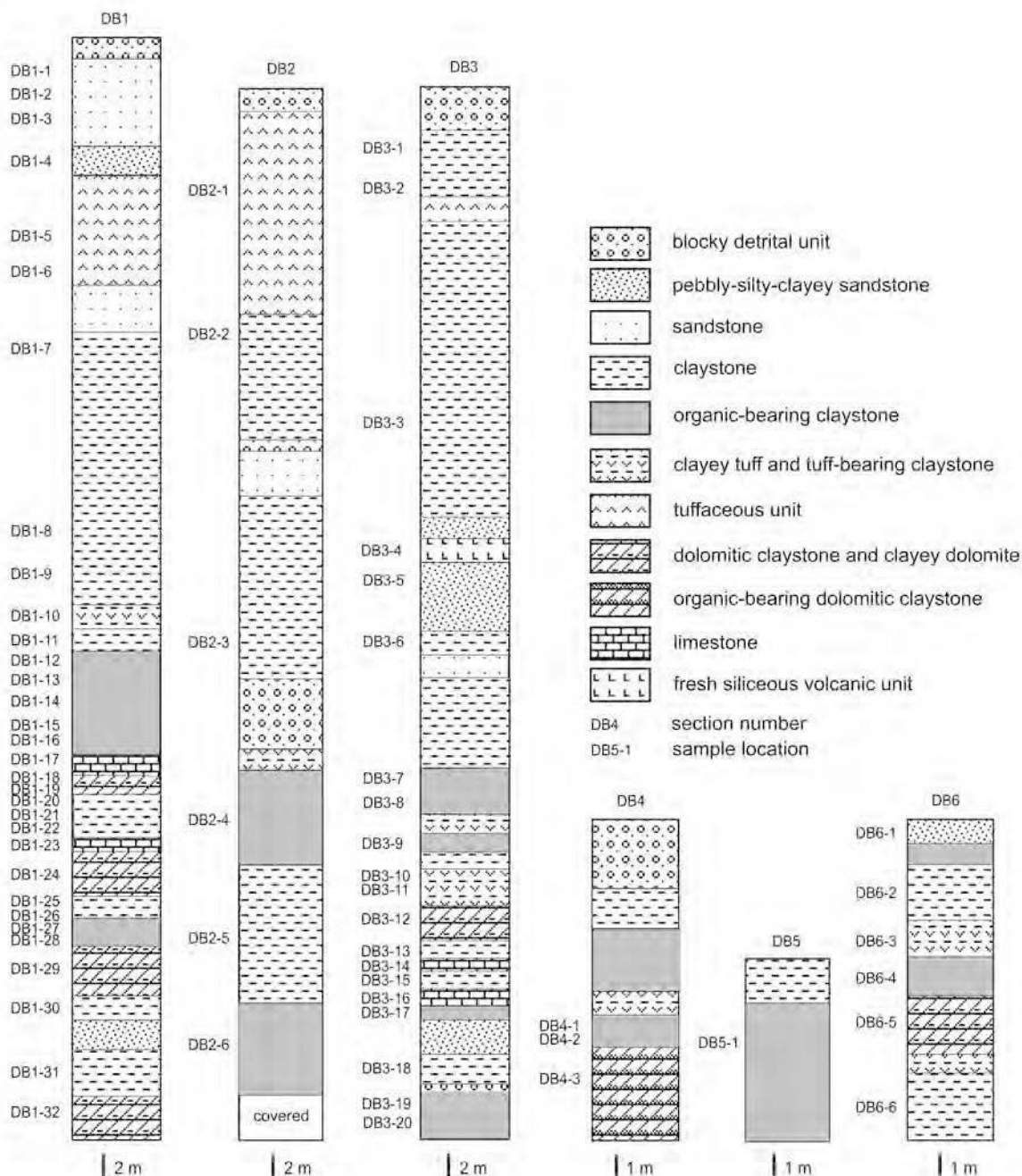

Figure 3. Distribution of the principal lithologies of the Doğanbey area (see Figure 1 for section locations, and Tables 1 and 2 for the mineralogical and chemical compositions of the samples, respectively).

Table 1. Mineralogical variation through stratigraphic sections of the Doğanbey area.

Sample	Rock type	smc	pal	ill	chl	kao	anl	fds	op	qtz	hbl	dol	cal
DB1-1	Sandstone	+		+	acc	acc		++	++		acc		
DB1-4	Clayey pebbly sandstone	+		acc	acc			+++	acc	+			
DB1-5	Tuffaceous unit	+		+				+	+	+	+		
DB1-6	Tuffaceous unit	+				acc		+	+	+	+		
DB1-7	Sandy, silty claystone	+++				+		acc	+	+			
DB1-8	Sandy, silty claystone	+++		acc	acc	+		+	+	+		+	
DB1-9	Sandy, silty claystone	+++			?	?	acc	+	+	+			
DB1-10	Clayey tuff	++		acc		acc		acc	acc	+		acc	
DB1-11	Claystone	+++		+		+		acc	acc	+			
DB1-13	Organic-bearing claystone	+++		acc		acc		+	+	+			
DB1-14	Organic-bearing claystone	+++		acc		acc		+	acc	acc		acc	
DB1-15	Organic-bearing claystone	+++	++										
DB1-16	Organic-bearing claystone	+++	++										
DB1-17	Limestone	acc											+++++
DB1-18	Claystone	+++		acc		acc				+			
DB1-20	Sandy, silty claystone	++		acc					acc	+			+
DB1-21	Sandy, silty claystone	++++						acc		acc			
DB1-22	Sandy, silty claystone	+++		acc				acc	acc	acc	acc		
DB1-23	Limestone	acc								acc		acc	+++++
DB1-24	Clayey dolomite	++								acc		+++	acc
DB1-25	Sandy, silty claystone	++++		+				+		+		acc	
DB1-26	Sandy, silty claystone	++		acc				+	+	+		+	
DB1-27	Organic-bearing claystone	++++		acc		acc		acc		acc			
DB1-28	Organic-bearing claystone	++++	acc	acc		acc		acc	+	acc		acc	acc
DB1-29	Clayey dolomite	++								acc		+++	
DB1-30	Sandy, silty claystone	++		acc			acc	+	acc	+			
DB1-31	Sandy, silty claystone	+++		acc		acc		+		+	acc		
DB1-32	Clayey dolomite	++		acc		acc			acc	+		++	
DB2-1	Tuffaceous unit	acc		+				+	+	+	+		
DB2-2	Claystone	++++		acc				acc	acc	acc			
DB2-3	Sandy, silty claystone	++		acc		acc		+	+				
DB2-4	Organic-bearing claystone	++		acc				+	+	acc			
DB2-5	Claystone	+++		acc		+	acc	+	+				
DB2-6	Organic-bearing claystone	++		acc			acc	+	+	acc			

gradual transition to marl. Claystone beds are intercalated with silty and sandy, angular−partially angular pebbly and blocky beds. Pebbles comprise degraded tuffaceous fragments. The broken faces of the claystone are stained black locally. The claystone also contains intercalated, thick-laminated, lenticular carbonized roots and root imprints (DB3-8). The claystone becomes darker with increasing root-imprint content. The dark-brown claystone (DB5-1) has prevalent root imprints and carbonized root relics as well as thin shells of lacustrine lamellibranchs. This facies has gradual contacts with tuffaceous claystone−clayey tuff. Increase in tuffaceous fragments and carbonate sediments in the claystone produces green and white coloration, respectively.

Stratigraphically, organic-material lenses and root imprints bearing smectitic claystone increase downwards and basinwards, and thick beds of smectite and volcaniclastic units occur in the middle and upper parts of the sequence where volcaniclastic detrital units wedge out laterally basinwards.

Limestone-dolomite-marl

This is a white, cream-colored, variegated, dissolution-void-bearing holocrystalline limestone, locally hard (DB1-23), with detrital sediment and root imprints. Clayey carbonate units bear microcavities filled with calcite cement. Clayey dolomite−marl (DB3-12) is brown, white and cream-colored, and contains variable amounts of tuffaceous fragments and silty sediments. There are transitional contacts among limestone, clayey dolomite and marl in the study area.

Tuff

This is a pale-gray, dull-white, greenish-yellow, thick-laminated, poorly welded unit, having wavy

Table 1 (*contd.*)

Sample	Rock type	smc	pal	ill	chl	kao	anl	fds	op	qtz	hbl	dol	cal
DB3-1	Sandy, silty claystone	++		acc		+		+	+	acc			
DB3-2	Claystone	+++		acc		+	acc		+	acc			
DB3-3	Sandy, silty claystone	++		acc		+		+	+	acc			
DB3-4	Siliceous volcanic unit						acc		++++				
DB3-5	Pebbly sandstone	+		acc				+	+	+	acc		
DB3-6	Claystone	+++++		acc		acc							
DB3-7	Organic-bearing claystone	+++++		acc				acc		acc			
DB3-8	Organic-bearing claystone	+++		acc				+		+			
DB3-9	Organic-bearing claystone	+++		acc	acc			acc	+	+			
DB3-10	Tuff-bearing claystone	+++		acc		acc	acc	acc	+	+			
DB3-11	Tuff-bearing claystone	+++	acc	acc			acc	+	acc	+			
DB3-12	Clayey dolomite	+		acc						acc		+++	+
DB3-13	Sandy, silty claystone	+++		acc		acc		+		acc			
DB3-14	Limestone	acc		acc				acc		acc			++++
DB3-15	Claystone	+++		+		acc		acc	+	+			
DB3-16	Limestone	acc		acc						acc			++++
DB3-17	Organic-bearing claystone	++++		acc			acc	acc	+	acc			
DB3-18	Sandy, silty claystone	+++		acc		+		+		+			
DB3-19	Organic-bearing claystone	++++		acc		acc			acc	acc			
DB3-20	Organic-bearing claystone	+++		acc				acc	acc	acc	acc		
DB4-1	Organic-bearing claystone	++++						acc	acc	acc			
DB4-2	Organic-bearing claystone	++++		acc						acc		+	+
DB4-3	Organic-bearing dolomitic claystone	++		acc				acc	acc			++	+
DB5-1	Organic-bearing claystone	+++++		acc					acc	acc			
DB6-1	Clayey pebbly sandstone	+		acc		+		+	+	+			
DB6-2	Claystone	+++++		acc									
DB6-3	Clayey tuff	+++		acc		acc		+	+	+			acc
DB6-4	Organic-bearing claystone	++++		acc		acc		acc	acc	acc			
DB6-5	Clayey dolomite	+		acc				acc		acc		+++	
DB6-6	Claystone	+++		+		acc		acc	+	+			

smc − smectite, pal − palygorskite, ill − illite, chl − chlorite, kao − kaolinite, anl − analcime, fds − feldspar, op − opal-ct, qtz − quartz, hbl − hornblende, dol − dolomite, cal − calcite, + − relative abundance of mineral, acc − accessory.

character locally. The tuffaceous unit is generally coarse- to fine-grained, and is altered in places to clayey tuff and tuffaceous claystone. Tuffaceous units have prevalent voids, and contain mostly altered volcanic pebbles and altered-andesitic blocks. This unit is highly altered and has gradual transitions with feldspar-crystal and minor glass-shard-bearing units. Tuffaceous units are Fe-oxidized and oxhydroxidized in places.

Sandstone-mudstone-conglomerate

This consists of pale yellowish-gray and green, medium hard, fine- to medium-grained sandstone layers and lenses, intercalated or alternating with minor sub-rounded-pebble-bearing, medium-to-coarse-grained sandstone. Sandstone layers are 20 cm to 2 m thick. These units also alternate with 1−2 m thick, yellow to orange tuff and intercalated mudstone, and wedge out basinwards. Sandstones also alternate with silty and sandy claystone layers repeated several times due to climatic change. Sandstone comprises quartz, mafic minerals, and accessory biotite, cemented by sandy, silty and clayey sediments; thus, it is characterized as tuffaceous and clayey sandstone, and also bears root imprints. This sedimentary environment was followed by deposition of pebbly levels and lenses, composed of yellowish, poorly to moderately cemented coarse to very

Table 2. Major-element and trace-element compositions of various lithologies of the study area (see Table 1 for the mineralogical compositions of the samples).

Major oxides (wt.%)	Fresh samples					Altered samples					
	DB1-5	DB1-6	DB2-1	DB3-4	DB3-5	DB1-8	DB1-13	DB1-25	DB1-26	DB2-4	DB3-1
SiO_2	64.14	62.38	66.65	68.86	63.0	60.67	62.5	59.5	52.7	60.5	60.03
Al_2O_3	15.53	15.39	15.66	7.12	16.0	15.27	15.8	13.3	11.8	16.5	16.21
Fe_2O_3*	3.96	4.42	2.76	6.15	6.0	5.51	6.0	4.5	5.1	8.1	5.07
MgO	1.42	0.97	1.00	0.24	0.9	0.99	1.4	2.5	5.5	0.8	0.62
CaO	2.69	1.67	3.12	0.29	2.3	1.64	2.6	4.3	7.7	1.9	1.15
Na_2O	2.32	1.73	3.40	0.42	1.3	1.49	1.5	1.1	1.1	1.0	1.25
K_2O	2.80	2.56	3.44	1.61	2.2	2.45	2.4	2.2	2.1	2.1	2.85
TiO_2	0.60	0.62	0.34	0.92	0.9	0.77	0.9	0.1	0.1	0.1	0.90
P_2O_5	0.12	0.23	0.15	0.45	0.1	0.14	0.1	0.7	0.9	1.2	0.12
MnO	0.06	0.04	0.06	0.02	0.1	0.08	0.1	0.1	0.1	0.1	0.04
LOI	5.9	9.5	2.9	13.3	6.1	10.6	5.6	11.7	12.7	7.3	11.3
Sum	99.54	99.52	99.48	99.38	98.9	99.62	98.9	100	99.7	99.6	99.55
Trace elements (ppm)											
Ba	1195.4	1451.6	1180.1	1704.1	741.6	958.1	723.7	670.5	745.0	615.6	916.8
Be	3	2	3	1	3	2	2	1	2	1	2
Co	7.2	3.8	5.0	4.9	8.3	12.7	9.1	6.7	9.6	11.9	15.1
Cs	4.8	6.9	7.7	1.2	6.3	6.7	6.8	5.8	5.6	6.5	9.8
Ga	18.8	18.3	18.7	8.4	19.2	19.3	18.8	16.1	15.6	17.7	18.4
Hf	4.9	4.9	4.4	6.6	5.1	6.3	4.7	5.3	7.5	6.9	8.4
Nb	17.5	15.4	18.0	11.4	16.3	17.4	15.2	13.5	16.6	17.7	23.4
Rb	89.8	96.4	163.1	13.1	96.9	102.4	111.7	103.5	94.8	92.3	125.7
Sr	681.3	713.3	757.7	615.6	512.4	514.9	393.7	432.8	485.9	499.4	581.0
Ta	1.4	1.3	1.4	1.1	1.5	1.6	1.3	1.2	1.5	1.8	2.2
Th	19.5	19.4	21.0	28.5	22.3	22.8	21.9	18.4	17.2	23.3	30.0
V	89	111	42	188	92	126	79	94	136	122	148
W	2.6	3.8	1.6	4.3	2.9	3.6	1.9	2.3	2.6	3.2	4.0
Zr	169.3	164.0	141.7	212.2	184.7	217.4	165.0	177.4	272.5	225.6	290.2
Y	19.5	18.6	17.3	13.6	21.2	23.4	20.4	16.0	32.7	23.4	27.5
Cu	12.3	12.6	22.9	215.4	11.4	13.8	11.2	17.1	10.4	13.8	18.4
Pb	13.6	34.3	8.2	18.4	16.0	18.6	11.7	10.2	15.1	15.2	26.0
Zn	17	14	40	11	38	34	39	30	29	38	43
Ni	5.1	3.0	4.6	9.3	11.9	12.5	12.1	25.2	35.1	12.2	14.1
Cr	40	40	20	20	20	60	60	60	60	60	60
As	2.7	15.9	0.6	91.3	3.3	6.4	1.5	0.8	1.2	4.9	3.1
Cd	0.1	0.1	0.1	0.1	0.1	0.1	0.1	0.1	0.1	0.1	0.2
Sb	0.1	0.1	0.1	2.7	0.1	0.2	0.1	0.1	0.1	0.1	0.1
Bi	1.4	2.2	0.1	14.1	1.2	1.3	0.6	0.5	0.7	1.7	1.4

* all Fe as Fe_2O_3

coarse sands and pebbles, which were related to climatic and stream-ingression changes. The pebbles consist of andesitic tuffaceous fragments, having diameters ranging from a few mm to 10−15 mm. Depositional and structural features indicate that the area was affected by small-scale to major normal faults which developed in the central Anatolian tectonic regime (Umut *et al.*, 1987; Şenel, 2002).

RESULTS

Petrographical determinations

Tuffaceous units are composed mainly of twinned and locally zoned intermediate plagioclase, hornblende (in places exhibiting prismatic cleavage, chloritization and Fe oxidation), and traces of K-feldspar phenocrysts (showing evidence of alteration) (Figure 4a−d). These phenocrysts are surrounded by isotropic, amorphous, volcanic-glassy material and fine-grained crystals of feldspar and hornblende.

In sample DB1-19, subrounded to irregular clayey granules and fractures are cemented by microsparitic to sparitic meniscus calcite cement (on the basis of XRD and EDX analyses), interpreted as evidence of brecciation due to calcretization (Figure 4e) (cf. Tucker and Bathurst, 1990; Wright and Tucker, 1991; and Karakaş and Kadir, 1998). The size of the calcite crystals increases toward the centers of pores and fractures. In sample DB1-28, the development of microsparitic carbonate cement in spaces or fractures subparallel to

Table 2 (*contd.*)

Major oxides (wt.%)	— Altered samples —			—— Highly altered samples ——				Carbonate-organic-bearing claystone samples			Carbonate sample
	DB3-3	DB3-9	DB6-1	DB1-16	DB4-1	DB5-1	DB6-4	DB4-3	DB4-2	DB1-24	DB1-23
SiO$_2$	58.62	58.5	58.16	51.09	53.15	40.40	43.83	26.75	41.07	34.15	5.98
Al$_2$O$_3$	15.78	14.3	15.33	11.18	15.22	9.74	12.26	4.97	11.38	7.48	1.37
Fe$_2$O$_3$*	6.03	8.5	5.10	3.73	4.53	3.11	3.92	1.77	3.89	3.33	0.80
MgO	0.78	2.4	1.53	5.48	2.89	5.98	4.49	10.44	6.05	7.76	0.80
CaO	1.30	3.6	1.06	1.10	1.36	8.49	4.72	20.69	6.85	15.13	49.89
Na$_2$O	1.05	0.5	1.10	0.31	0.70	0.19	0.23	0.24	0.24	0.34	0.06
K$_2$O	2.14	2.2	2.74	1.09	2.03	0.63	0.88	0.41	0.80	1.04	0.23
TiO$_2$	0.82	0.1	0.78	0.38	0.59	0.30	0.37	0.19	0.32	0.33	0.07
P$_2$O$_5$	0.15	1.0	0.08	0.09	0.09	0.11	0.10	0.17	0.12	0.07	0.08
MnO	0.06	0.9	0.04	0.09	0.04	0.05	0.07	0.06	0.10	0.01	0.06
LOI	12.9	7.9	13.7	25.3	19.1	30.9	29.0	34.2	29.0	30.2	39.9
Sum	99.64	99.9	99.63	99.85	99.71	99.91	99.88	99.89	99.84	99.86	99.22
Trace element (ppm)											
Ba	830.4	419.3	858.1	373.9	651.8	324.0	306.1	370.9	468.7	295.4	5060.6
Be	2	4	2	1	2	1	2	1	1	1	1
Co	10.5	14.9	8.6	8.6	9	6.3	9.6	4.4	9.5	8.6	2.3
Cs	6.2	8.5	9.8	5.4	8.6	7.8	10.4	6.5	9.8	3.8	0.8
Ga	18.3	17.6	18.7	13.1	17.4	12.2	13.5	5.4	13.8	9.2	1.9
Hf	6.0	4.5	4.4	2.5	3.7	2.3	2.6	1.1	2.3	2.1	0.5
Nb	16.1	18.6	17.3	8.4	12.9	7.3	8.5	4.0	7.8	7.3	1.4
Rb	84.2	141.0	125.7	79.5	105.9	51.4	61.3	25.7	60.7	54.1	14.3
Sr	474.0	274.9	305.4	164.5	238.3	272.4	205.7	438.3	273.7	384.5	131.2
Ta	1.5	1.4	1.5	0.7	1.2	0.6	0.7	0.3	0.8	0.6	0.2
Th	22.0	15.1	22.7	12.2	21.1	8.4	12.3	4.2	11.2	7.8	1.6
V	129	129	101	82	71	90	91	35	76	73	18
W	3.1	1.9	3.0	1.2	2.0	1.2	1.8	0.8	1.6	1.0	0.1
Zr	207.3	161.7	146.0	81.0	112.7	82.6	83.7	39.8	79.5	73.2	13.1
Y	24.1	23.7	15.5	10.3	15.0	12.0	18.9	7.6	23.8	8.3	3.7
Cu	16.6	16.2	8.1	10.7	9.8	18.6	18.0	5.1	24.9	19.4	3.3
Pb	23.9	9.2	18.2	10.0	16.5	10.6	15.0	6.2	16.1	4.6	2.5
Zn	31	55	38	35	40	33	35	23	47	23	10
Ni	10.6	151.2	7.7	29.5	12.0	15.3	22.7	11.9	19.7	60.4	14.4
Cr	70	60	50	50	50	50	50	30	160	70	30
As	8.9	2.1	20.4	0.9	1.1	8.6	7.7	2.5	1.0	1.0	0.7
Cd	0.1	0.2	0.1	0.1	0.1	0.1	0.1	0.2	0.2	0.1	0.3
Sb	0.1	0.1	0.2	0.1	0.2	0.2	0.3	0.2	0.3	0.1	0.1
Bi	1.7	0.4	1.2	0.4	0.9	0.5	0.9	0.3	0.9	0.2	0.1

all Fe as Fe$_2$O$_3$

elongated, irregular clay matrix is also evidence of diagenesis during or following calcretization (Figure 4f). Thus, in clayey dolomite of sample DB1-29, intergrowths of micritic dolomite with clay minerals are associated with organic material (Figure 4g).

Limestone sample DB1-17 is composed of needle-like calcite crystals having mutually parallel to subparallel orientations and contains accessory small black organic-material relics (Figure 4h). These calcite needles are ~0.2 mm long. Carbonate- and detritus-bearing claystone sample DB1-20 has prevalent bar-like structures resembling diatoms (Figure 4i).
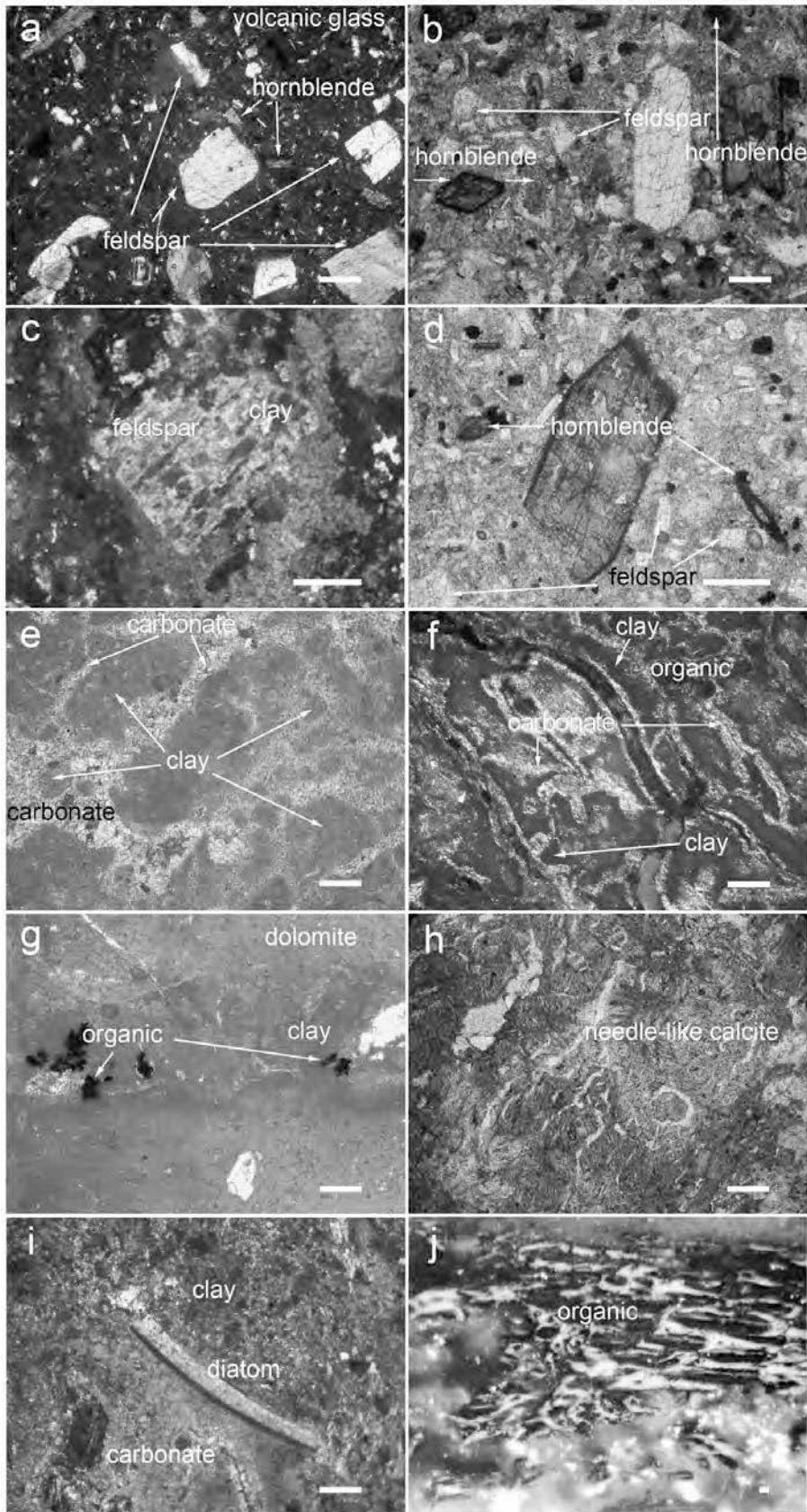
Polished-section observations show that roots are locally partially converted to carbonized organic material in some samples (Figure 4j).

XRD determinations

The XRD analyses of bulk samples and clay fractions are given in Table 1 and in Figures 5 and 6. Smectite is the prevalent alteration product associated with mainly plagioclase, hornblende, opal-CT and quartz, and accessory K-feldspar, illite, kaolinite, analcime and chlorite. Smectite is also accompanied either by minor palygorskite (samples DB1-15 and DB1-16), or accessory palygorskite (samples DB1-28 and DB3-11).

Calcite and dolomite occur either in association with smectitic claystone, such as detected in samples DB4-1, -2 and -3 (Figure 5), or as levels having transitional contacts, as in samples DB1-23 and DB1-24.

Mineral assemblages are not vertically and laterally uniform. A slight inverse relationship between smectite
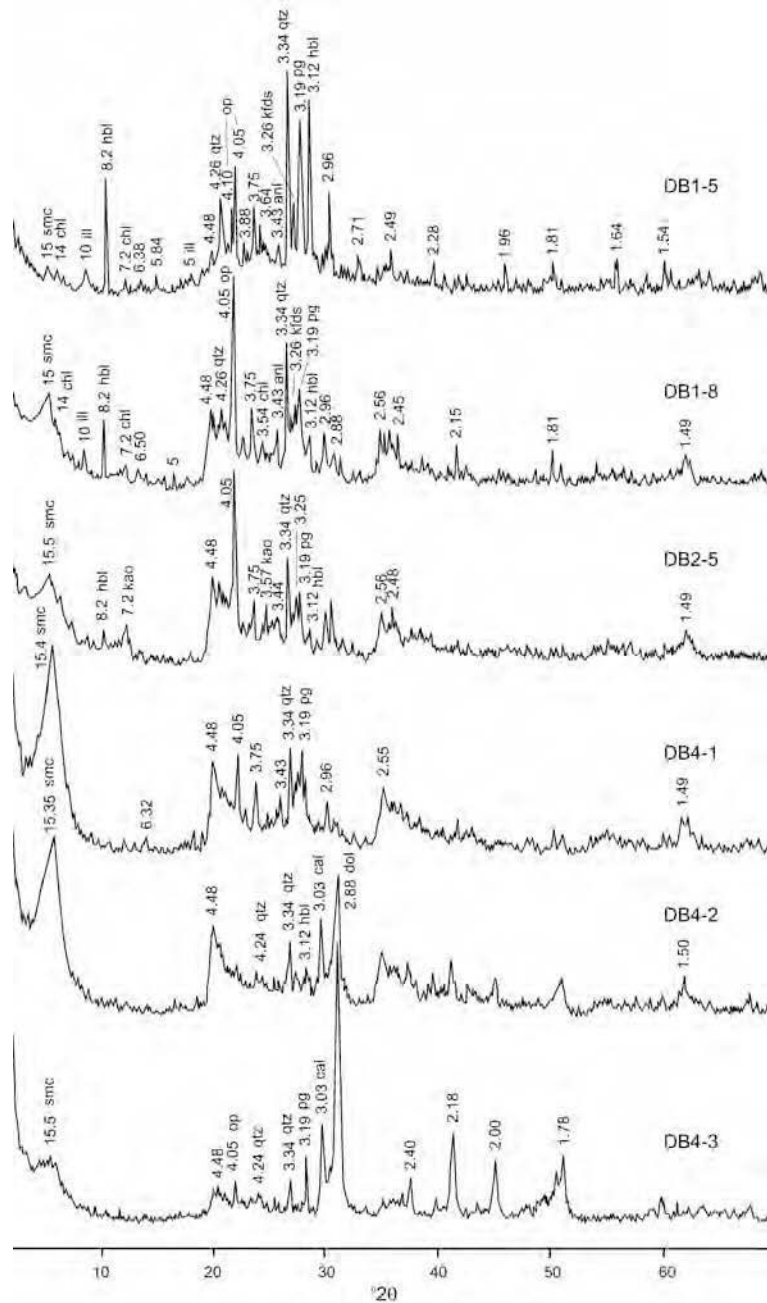
Figure 5. XRD patterns for Doğanbey bulk clayey materials. smc − smectite, ill − illite, chl − chlorite, kao − kaolinite, anl − analcime, pg − plagioclase, kfds − K-feldspar, hbl − hornblende, qtz − quartz, op − opal-CT, dol − dolomite, cal − calcite. CuKα radiation.

Figure 4 (*facing page*). Photomicrographs of: (a) feldspar phenocrysts (plagioclase, in part twinned or zoned) in a matrix of glass and microlites, under crossed-polarized light (DB1-1), scale bar = 0.25 mm; (b) phenocrysts of altered feldspar and black-rimmed hornblende in a matrix of glass with feldspar microlites, under plane-polarized light (DB1-5); (c) resorbed feldspar altered to clay minerals, under plane-polarized light (DB1-5); (d) Fe oxide-rimmed and partially chloritized hornblende crystal, under plane-polarized light (DB1-5); (e) development of microsparitic to sparitic meniscus cement between clayey granules, under plane-polarized light (DB1-19); (f) development of microsparitic to sparitic cement in pores or fractures subparallel to long, irregular clayey materials, under plane-polarized light (DB1-28); (g) subparallel to parallel needle-like calcite crystals associated with relics of black organic material, under plane-polarized light (DB1-17); (h) relationship between micritic dolomite, clay and organic materials in clayey dolomite, under plane-polarized light (DB1-29); (i) bar-like diatom in carbonate- and detritus-bearing-clayey materials, under plane-polarized light (DB1-12); (j) polished-section photomicrograph of carbonized organic material (DB6-4).

Figure 6. XRD patterns for Doğanbey clay fractions. (A) smectite (DB5-1); (B) smectite+palygorskite (DB1-16). (a − powder, b − oriented, c − ethylene-glycol solvated, d − heated to 350ºC, e − heated to 550ºC). smc − smectite, pal − palygorskite, pg − plagioclase, qtz − quartz, op − opal-CT. CuKα radiation.

and feldspar was observed; thus, an increase in smectite is accompanied by a decrease in feldspar, and *vice versa*. Conversely, smectite+palygorskite correlates positively with dolomite and negatively with calcite.

Smectite has sharp basal reflections varying between 15 and 15.5 Å which expand to ~17 Å with ethylene-glycol treatment and collapse to 10.2 Å and 9.9 Å after heating at 350ºC and 550ºC, respectively, for 2 h (Figure 6A). The d_{060} value of smectite is 1.49 Å, suggesting a dioctahedral character (Moore and Reynolds, 1989). Palygorskite was determined by its diagnostic basal reflection at 10.32 Å that was unaffected by ethylene-glycol treatment, but this peak,

together with a smectite peak in the same sample, moved to 10.5 and collapsed to 9.8 Å after heating at 350 and 550ºC, respectively, for 2 h (Figure 6B). Kaolinite was recognized at 7.16 and 3.57 Å, and the 7.16 Å peak was not affected by ethylene-glycol treatment, but reduced and then collapsed upon heating at 350 and 550ºC, respectively (Figure 5). The occurrence of peaks at 10.24 Å following treatment with DMSO is related to the presence of traces of kaolinite (Moore and Reynolds, 1989). Chlorite was determined by 14.2 and 7.2 Å reflections, and by the fact that it was unaffected by ethylene-glycol treatment and heating at 550ºC. Analcime was defined by peaks at 3.43, 5.60 and

Figure 7 (*facing page*). SEM images of: (a,b) regular growth of smectite flakes as the matrix between sedimentary grains (DB4-1); (c,d) highly resorbed feldspar crystals (DB2-4), (e) relict dolomite rhombs enclosed by palygorskite fibers (DB1-16); (f) volcanic glass enclosed by dolomite-bearing palygorskite matrix (DB1-16); (g) suboriented irregular kaolinite plates showing slumping (DB2-5); (h,i) rod-, ellipsoidal sphere- and sieve-like diatoms (DB2-6).

2.92 Å. Hornblende was distinguished by diagnostic reflections at 8.2 and 3.12 Å, plagioclase by 3.19 Å, K-feldspar by 3.25 or 3.26 Å, and opal-CT by 4.05 and 4.10 Å (Figure 5). The abundance of opal-CT was also observed in sample DB3-4 (Figure 5). Increase in the XRD background in most of the samples may indicate the presence of opal-A, as reported elsewhere (Jones and Segnit, 1971; Iijima and Tada, 1981).

SEM-EDX analyses

Scanning electron microscopy analyses indicate that alteration products such as smectite and smectite+palygorskite were present as a matrix between feldspar, glass shards, hornblende and quartz (Figure 7a,b). Smectite is associated with relict feldspars that have mosaic-like form caused by dissolution and degradation (Figure 7c,d). Smectite flakes occur as regular pore- and fracture-fillings and as grain coatings. The crystal size of smectite increases from the pore and fracture margins towards their centers, and flaky smectite plates are rimmed by fibrous palygorskite (Figure 7a,b). Palygorskite has also developed as a matrix on and between relict carbonate rhombs and, in a few cases, encloses relict volcanic glass (Figure 7e,f). Palygorskite fibers are ~2 μm long. In sample DB2-5, kaolinite exhibits irregular plates that are roughly subparallel, indicating that the book-like or subparallel kaolinite plates were partly degraded and folded (after precipitation) due to slumping during or after tectono-sedimentation (Figure 7g).

Rod- (100 μm × 12 μm), ellipsoidal sphere- (12 μm × 10 μm), and sieve-like structures resembling diatoms have been observed and constitute a source for amorphous material in the alteration product, as determined by XRD (Figures 7h,i). The sieve-like structures are broken and altered. All of these diatom-like structures are surrounded by secondary phases.

The EDX spectra of smectite flakes exhibit strong peaks for Si followed by Al and Mg peaks in sample DB5-1, similar to the palygorskite spectra in sample DB1-16 in which only the intensity of Al is slightly stronger and Mg weaker in the smectite than in the palygorskite. An EDX analysis of resorbed mosaic-like relict feldspar crystals exhibits strong peaks for Si, followed by Al, and weaker ones for Ca and Na. Rhombic crystals between palygorskite fibers show strong peaks for Ca and Mg (suggesting a dolomitic composition), and subrounded-, rod- and sieve-like diatoms yielded very strong peaks for Si. The black volcanic-glass shards exhibit a strong peak for Si followed by smaller peaks for Al, Mg and Fe, and faint peaks for K, Ca, Na and Ti.

Geochemistry

Representative chemical analyses of fresh, altered, and highly altered samples, carbonate-bearing claystone and carbonate sediments are given in Table 2. The increase in LOI is an important indicator of progressive alteration and the presence of accompanying carbonate minerals and organic material.

Fresh and altered to highly altered volcanic rocks and carbonate-bearing claystone samples plot near the junction or borders of the andesitic, trachyandesitic, rhyolitic and alkali basalt fields (Figure 8) on the Zr/TiO_2 *vs*. Nb/Y diagram of Winchester and Floyd (1977). However, Zr, Ti, Nb and Y may be mobile under certain conditions (Hynes, 1980; Murphy and Hynes, 1986). Thus, it is suggested that the precursor material of the Doğanbey volcaniclastics was trachyandesitic and possibly rhyolitic in composition.
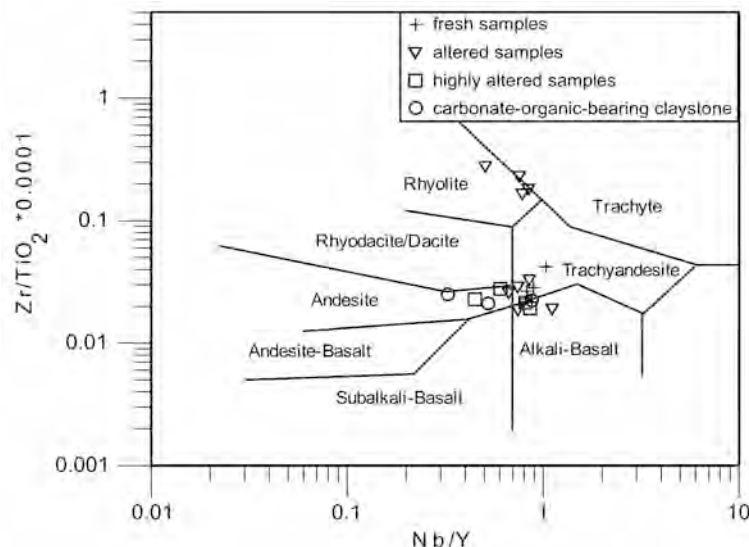

Figure 8. Discrimination of the Doğanbey area volcaniclastic rock samples using a Nb/Y- Zr/TiO_2 immobile element diagram (Winchester and Floyd, 1977).

Using gains and losses of mass (MacLean and Kranidiotis, 1987), enrichments and depletions of major and trace elements from fresh (DB1-5, DB1-6, DB3-4, and DB3-5), to altered, to highly altered samples and carbonate- and organic-matter-bearing claystone units were observed (Table 3; Figure 9).

These chemical changes reflect the mineralogy and crystal chemistry of clays and associated volcaniclastic rocks (Tables 2 and 3). Si, Na, K, Sr, Rb and Ba have been depleted during the alteration of K-feldspar and plagioclase. Conversely, Mg, Ca, Fe (except in highly altered samples) and Ni have been relatively enriched by alteration of ferromagesian minerals (*e.g.* hornblende, biotite and certain glasses) and material derived from basement ophiolitic and dolomitic units. The alkaline composition of the fluid phase, due to gain of Ca (Christidis and Scott, 1997) controlled by high evapora-tion and relative increase of Al/Si ratio and Fe with advance of alteration, caused precipitation of smectite, along with palygorskite with increasing Mg downwards. The release of silica during the alteration process resulted in the development of small amounts of opal-CT. Ti is consistently leached through all stages of alteration, similar to the case reported by Zielinski (1982), in contrast to Christidis (1998) who considered this element to be relatively immobile during alteration (*e.g.* in bentonite formation). Mg and Ca are situated in dolomite and calcite, and K in illite and − to a lesser extent − in the interlayer sites of smectite.

Most of the trace elements in the carbonate rocks (DB1-23) have smaller concentrations compared to the volcaniclastic rocks, except for Ba (5060.6 ppm) which is extremely high (Table 2). Ba and Rb tend to occur in K-bearing phases, such as K-feldspar, and to some extent

Table 3. Mass gains and losses (g, ppm) from the Beyşehir area samples (based on 100 g of average fresh rock composition and constant Al_2O_3).

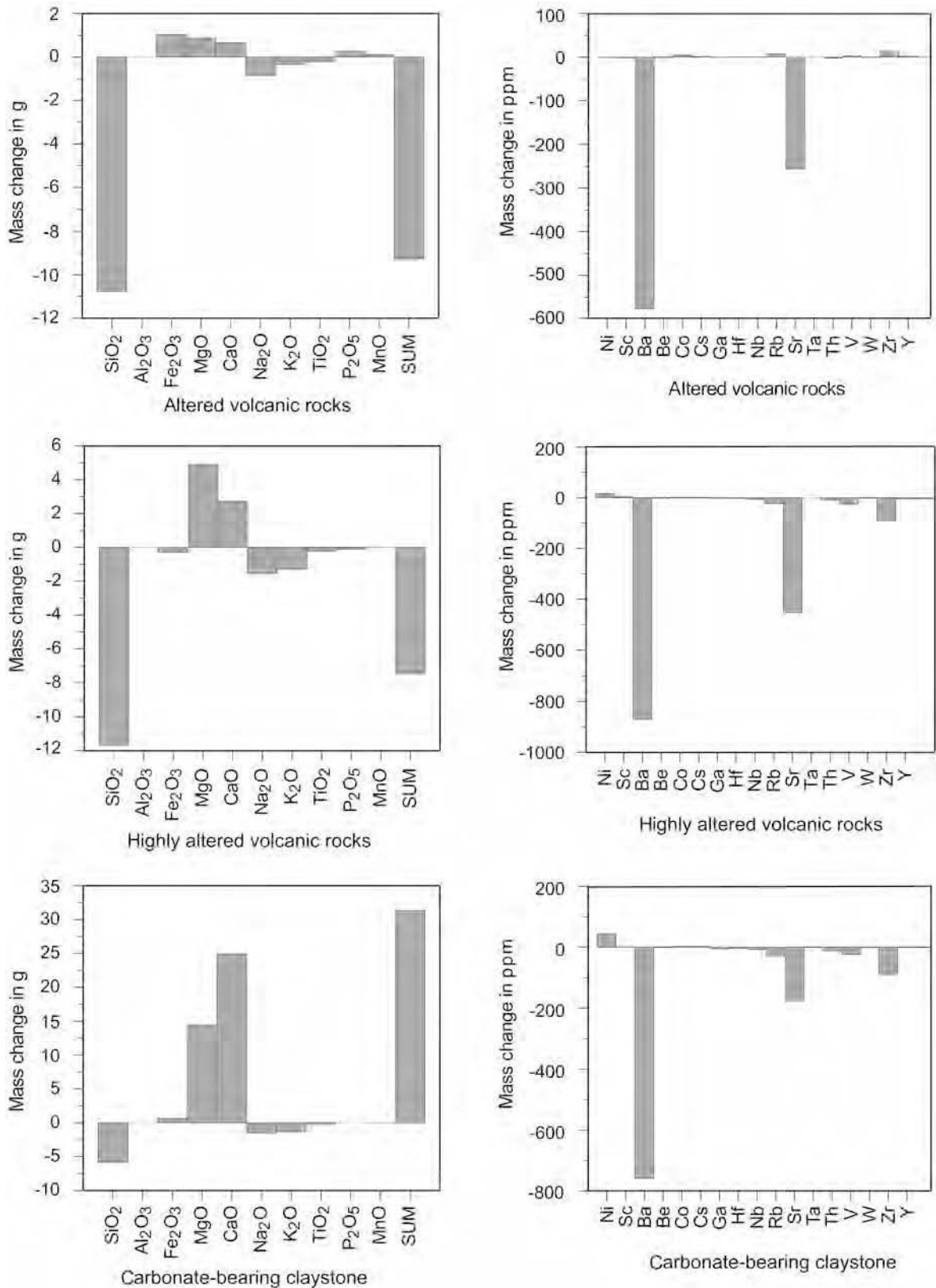|	Altered samples	Highly altered samples	Carbonate-organic-bearing claystone samples
	$n = 9$	$n = 4$	$n = 3$
Major oxides (g)			
SiO_2	−10.77	−11.67	−5.86
Al_2O_3	−0.01	0.00	−0.01
ΣFe_2O_3	1.02	−0.28	0.65
MgO	0.88	4.92	14.46
CaO	0.66	2.72	24.98
Na_2O	−0.86	−1.55	−1.48
K_2O	−0.35	−1.29	−1.31
TiO_2	−0.22	−0.22	−0.20
P_2O_5	0.27	−0.11	0.00
MnO	0.11	0.02	0.05
Sum	−9.27	−7.45	31.30
Trace elements (ppm)			
Sc	−2.05	3.31	2.71
Ba	−575.31	−871.40	−757.75
Be	−0.59	−1.01	−1.09
Co	4.15	1.91	4.01
Cs	1.24	2.07	3.42
Ga	−0.50	−3.68	−4.25
Hf	0.26	−2.61	−2.77
Nb	−0.01	−7.13	−7.36
Rb	7.07	−22.88	−30.36
Sr	−256.62	−452.22	−176.10
Ta	0.07	−0.60	−0.60
Th	−2.64	−9.64	−11.98
U	−3.08	−2.06	−6.08
V	2.87	−27.11	−23.86
W	−0.46	−1.61	−1.55
Zr	13.45	−91.08	−90.12
Y	2.80	−5.04	−0.66
Cu	−42.26	−41.71	−33.30
Ni	21.52	11.62	33.49
As	−17.79	−18.53	−20.79
Cd	0.02	0.03	0.18
Sb	−0.50	−0.41	−0.34
Bi	−2.84	−3.18	−3.19

Figure 9. Mass change of the major elements (g) and trace elements (ppm) in the study area.

Table 4. Chemical compositions (wt.%) and structural formulae for pure smectite samples.

Major oxides (wt.%)	DB1-21	DB2-2	DB3-7	DB5-1	DB6-2
SiO_2	58	56.5	55.8	54.5	53.6
Al_2O_3	20.5	22	20	19.5	21.5
ΣFe_2O_3	4.5	5	5.6	5.5	4.6
MgO	1.2	1	0.5	1.5	1
CaO	0.6	0.8	0.8	0.5	0.6
Na_2O	0.3	0.2	0.5	0.3	0.5
K_2O	0.5	0.8	0.5	0.6	0.5
MnO	0.1	0.1	0.1	0.05	0.1
TiO_2	0.5	0.5	0.5	0.3	0.3
LOI	13.5	13	15.6	17.15	17.2
Structural formulae based on 22 oxygen atoms					
Tetrahedral					
Si	7.91	7.7	7.84	7.8	7.66
Al	0.09	0.3	0.16	0.2	0.34
Octahedral					
Al	3.21	3.23	3.15	3.09	3.28
Fe	0.46	0.51	0.59	0.59	0.5
Mg	0.25	0.2	0.11	0.32	0.22
Mn	0.02	0.02	0.02	0.01	0.02
Ti	0.05	0.05	0.05	0.03	0.03
Interlayer					
Ca	0.09	0.12	0.12	0.08	0.09
Na	0.08	0.05	0.14	0.08	0.14
K	0.09	0.14	0.09	0.11	0.09
Octahedral charge	0.25	0.14	0.32	0.18	0.06
Total layer charge	0.34	0.44	0.48	0.38	0.40
Interlayer charge	0.35	0.43	0.47	0.35	0.41
x_t/x_o*	0.36	2.14	0.50	1.11	5.67

*: x_t/x_o, tetrahedral charge/octahedral charge ratio

hornblende, whereas Sr occurs in K- and Ca-bearing minerals, such as K-feldspar, Ca-plagioclase and carbonate minerals (except for sample DB3-4, which is composed mainly of amorphous volcanic matter).

Zirconium is immobile in partly altered samples, but has been released and mobilized from smectitic and carbonate- and organic-material-bearing smectite beds. Conversely, Nb is mobile and thus tends to be leached, with leaching paralleling the degree of alteration. Ni is enriched in the altered rocks relative to their counterparts, possibly due to contamination of ferromagnesian materials or to derivation from ophiolitic basement rocks.

The structural formulae of smectite were calculated from chemical analyses of clay fractions (Table 4). Al^{3+} (3.09−3.28) is the abundant octahedral cation and substitutes for Si cations in tetrahedral sites (0.09−0.34). Fe^{3+} (0.46−0.59), Mg (0.11−0.32), Mn (0.01−0.02) and Ti (0.03−0.05) substitute for octahedral Al^{3+}. By means of plotting on the Mg-Al-Fe ternary diagram, the smectite is shown to be beidellite (Güven, 1988; Figure 10). The tetrahedral and octahedral charges of smectites in the Doğanbey volcaniclastics are in the ranges 0.09−0.34 and 0.06−0.32, respectively, and their tetrahedral charge/octahedral charge (x_t/x_o) ratios are
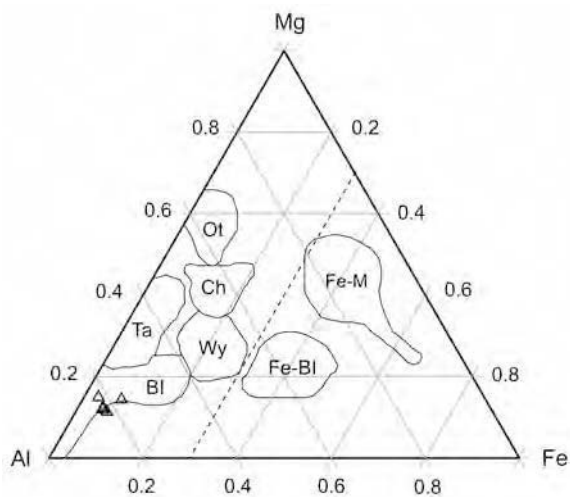

Figure 10. Ternary diagram of the main octahedral cations for smectites from the Doğanbey area (Güven, 1988). Ta − Tatatilla montmorillonite, Ot − Otay montmorillonite, Ch − Cheto montmorillonite, Wy − Wyoming montmorillonite, Fe-M − Fe-rich montmorillonite, BI − beidellite, Fe-BI − Fe-rich beidellite. The dashed line separates the Fe-rich smectites.

Table 5. Oxygen and hydrogen isotopic compositions of smectite and smectite + palygorskite from the Doğanbey area.

Sample	Yield (%)	$\delta^{18}O$ V-SMOW (‰)	Wt.% H_2O	δD V-SMOW (‰)
DB1-16	12.2	+ 28.7	13	−109
DB5-1	12.2	+ 24.4	12	−104
DB6-2	10.3	+ 23.4	9	−104

between 0.36 and 5.67, respectively. These values reveal that samples DB2-2, DB5-1, and DB6-2 might be beidellite, while DB1-21 and DB3-7 are montmorillonite, based on the classification of Güven (1988).

Stable-isotope geochemistry of smectite and smectite+palygorskite

The oxygen- and hydrogen-isotopic compositions of the smectite (DB5-1, DB6-2) and smectite+palygorskite (DB1-16) samples are listed in Table 5, and plotted in Figure 11. The $\delta^{18}O$ and δD values range between +23.4 and +28.7‰, and between −104 and −109‰, respectively. These isotopic data fall close to the smectite line, indicating a weathering-related alteration process (Craig, 1961; Lawrence and Taylor, 1971, 1972) outside the magmatic field (Taylor, 1974). In contrast, hydrothermal clays which form at higher temperatures plot closer to the meteoric water line (Taylor, 1974, 1979). Therefore, the formation of the Doğanbey smectite and smectite + palygorskite can be attributed to alteration by meteoric waters, the availability of which was in turn controlled by climatic conditions. The high $\delta^{18}O$ and negative δD values indicate high evaporation and depletion of ^2H and enrichment of ^{18}O and, thus, equilibrium with heavy water similar to what was set forth by Baker and Golding (1992) and Torres-Ruiz et al. (1994). The relatively greater enrichment of ^{18}O and depletion of ^2H in the smectite+palygorskite sample (DB1-16) compared to the smectite samples indicate that the palygorskite formed in equilibrium with fluid slightly more affected by evaporation than by the formation of smectite (Torres-Ruiz et al., 1994). The association of organic matter with highly altered rocks and carbonate-bearing claystone reveals that the study area was suitable for the growth of temperate vegetation and was affected by local climatic changes; the heavy-isotopic compositions of meteoric waters in the basin were thus influenced, as suggested by Barnard and Cooper (1981).

DISCUSSION

The widespread Pliocene lacustrine volcaniclastic rocks of the Doğanbey formation in the Beyşehir region (central Anatolia) consist of alternations of claystone, diatomaceous carbonatic claystone, carbonate, trachyandesitic and possibly of rhyolitic tuffaceous units, sandy-silty claystone, sandstone, mudstone and conglomerate beds, which indicate periodic climatic changes. The
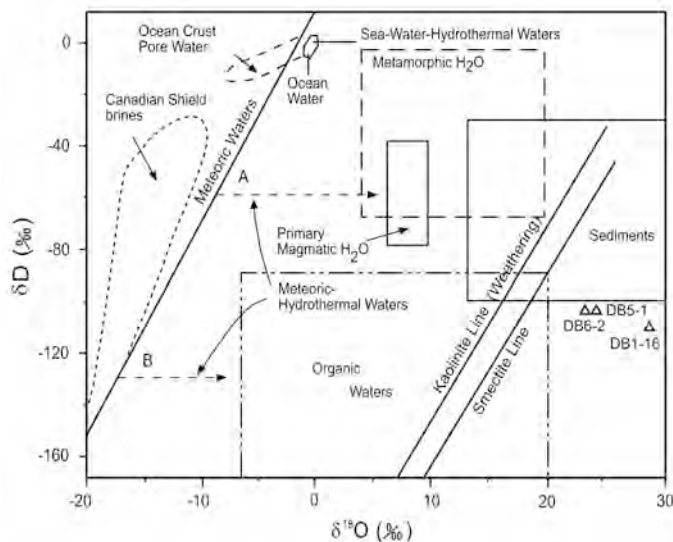

Figure 11. δD *vs.* $\delta^{18}O$ plot showing the isotopic compositions of smectites from the Doğanbey area (DB5-1, DB6-2) and smectite+palygorskite (DB1-16) (Sheppard, 1986). The line for kaolinite weathering is from Savin and Epstein (1970), and line for smectite is from Sheppard and Gilg (1996) and Yui and Chang (1999).
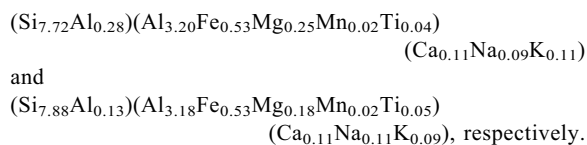
mineralogical assemblages are not vertically and laterally uniform, but correlations among mineralogical, chemical and lithological aspects are present. Smectite is prevalent in volcaniclastic units and claystone beds in the middle and upper parts of the sequence throughout the basin, and in organic-matter-bearing claystone beds in the lower part of the sequence and basinward. Smectite is accompanied by plagioclase, K-feldspar, opal-CT, hornblende, quartz and locally by dolomite, minor palygorskite, and accessory illite, kaolinite, analcime, chlorite and calcite. An increase of clayey and carbonate sediments downwards, and an increase of organic-material-rich lenses and root imprints associated with smectitic- and dolomitic-claystone basinward, indicate an anaerobic, swampy, shallow lacustrine depositional environment. Gradational transitions between organic-material-bearing dolomite and limestone levels — composed of needle-like calcite as intercalations between clayey tuffaceous units — indicate an environment of supersaturation caused by near-surface evaporation of solutions resulting in rapid precipitation of $CaCO_3$ as needle-like calcite (James, 1972; Knox, 1977; Wright, 1984). At thin-section scale, the development of microsparitic and sparitic meniscus calcite cement between subrounded and elipsoidal clay granules in association with root traces and other organic materials indicate that the environment of precipitation was subjected to oscillating wet and dry periods during which diagenesis operated and precipitation of clay minerals occurred (Wright and Tucker, 1991). Spaces between clayey granules and fractures developed in response to plant (root growth) activity, and by dessication during drought which followed wet periods (Mount and Cohen, 1984); therefore, the size of calcite crystals increases toward the center of the pores and fractures. Rod- and ellipsoidal sphere-like diatoms occur in sandy-silty claystone (samples DB1-20, DB2-6) due to periodic fresh-water supply to the environment of precipitation. Braiser (1985) reported that pennate diatom species require light and are limited to the photic zone during life and thus characterize fresh-water flux environments. The occurrence of diatoms in alteration products has been reported by Singer (1979), Galán and Ferrero (1982), Stamatakis *et al.* (1989), Altaner and Grim (1990), and Compton (1991).

Consumption of Ca due to precipitation of calcite and excess evaporation resulted in increasing Mg/Ca ratios that favored dolomitization during early diagenetic processes (Müller *et al.*, 1972; Ece and Çoban, 1994); a similar environment resulted in coprecipitation of smectite with the presence of Al and Fe released, in addition to Mg. The Mg required for dolomitization and palygorskite formation was possibly supplied by solutions derived from ophiolitic and carbonatic basement units of the study area. Subparallel increase of Mg contents with Ni and Co contents supports the idea that ophiolitic units were the Mg source (Table 2). Zedef *et*

al. (1994) also reported the Mg (18.43−34.17%), Ni (1853−2470 ppm), and Co (140−195 ppm) contents of a chromite deposit within ophiolitic units of the Beyşehir region.

Smectite is unstable in an Mg-prevalent environment, wherein it is partly transformed to palygorskite (Singer, 1989; Velde, 1995). The coexistence of clay minerals with micritic dolomitic sediments in association with organic materials, and the development of alteration products as a matrix between dolomite rhombs, were also determined at thin-section and SEM scales, respectively. Therefore, smectite seems to be associated with dolomite but not with calcite.

Textural and micromorphological images show that feldspar is generally extensively resorbed and volcanic glass devitrified due to fluid leaching. Skeletal feldspar and glass shards are etched by smectite, and hornblende is Fe oxidized and chloritized. The leaching of Na_2O and K_2O and decreasing Sr, Rb and Ba with increasing alteration, reveal that the hydration of volcaniclastic grains − such as feldspar (intermediate plagioclase) and hornblende, comprising high Al and minor amounts of Fe, in addition to volcanic glass − favored precipitation of beidellite and montmorillonite based on the x_t/x_o ratio of >1 for beidellite and <1 for montmorillonite (Güven, 1988) with these average structural formulae:

$$(Si_{7.72}Al_{0.28})(Al_{3.20}Fe_{0.53}Mg_{0.25}Mn_{0.02}Ti_{0.04})$$
$$(Ca_{0.11}Na_{0.09}K_{0.11})$$

and

$$(Si_{7.88}Al_{0.13})(Al_{3.18}Fe_{0.53}Mg_{0.18}Mn_{0.02}Ti_{0.05})$$
$$(Ca_{0.11}Na_{0.11}K_{0.09}), \text{ respectively.}$$

The δD and $\delta^{18}O$ values of the pure smectite and smectite+palygorskite samples fall close to the smectite line outside the magmatic field, indicating that these minerals may have formed from meteoric fluids which are controlled by the climatic conditions. Development of smectite as a matrix between volcaniclastics, and the gradual increase in smectite crystal size from degraded volcaniclastic grains dominated by feldspars and volcanic glass poreward, indicate an authigenic origin similar to that outlined by Christidis and Dunham (1997). Regular cornflake-type smectite in pores and fractures, and local, regular growth of palygorskite fibers at the edges of smectite plates (Inglès and Anadón, 1991; Rodas *et al.*, 1994; Colson *et al.*, 1998; and Jamoussi *et al.*, 2003) and as pore-bridging fibers between anhedral and subhedral dolomite rhombs (Weaver and Beck, 1977; Akbulut and Kadir, 2003) are further evidence which support *in situ* development of smectites by a partial dissolution-precipitation mechanism driven by chemical alteration of precursor feldspar and volcanic-glass shards during early diagenesis; and palygorskite by direct chemical precipitation from Mg-rich solutions coeval with or post-dating dolomitization and by transformation from smectite in the presence of Mg in a dry, quiescent-tectonic, alkaline lacustrine environ-

ment. A similar environment also resulted in the local precipitation of accessory analcime due to the release of Na from plagioclase, hornblende and volcanic glass. Leaching of alkalis and increase of Al/Si ratios due to enrichment in Al and depletion of Si resulted in the local formation of accessory kaolinite may well result from later weathering or circulation of acidic meteoric waters in the smectitic clays. The depletion of Si during or following the alteration process and the precipitation of smectite resulted in the formation of opal-CT.

CONCLUSIONS

Field observations and mineralogical and geochemical determinations reveal that beidellite- and montmorillonite-type smectites of the Doğanbey area (central Anatolia) mainly developed from Pliocene volcaniclastic rocks of the Doğanbey formation, comprising organic-matter-bearing claystone and tuffaceous and clastic units, whereas palygorskite formed in dolomitic inter-beds under alkaline, shallow swampy lacustrine depositional conditions controlled by periodic climatic changes. These climatic changes — of alternating influx of meteoric lacustrine fluid phases — are suggested by stable-isotope data (enrichment in δ^{18}O and depletion of δD) with a large evaporation factor for chemical alteration of metastable plagioclase and K-feldspar, devitrification of volcanic glass in volcaniclastic rocks which were deposited in the lake, as well as development of microsparitic to sparitic meniscus cement between clay and organic materials. Dissolution of precursor feldspar during early diagenesis resulted in depletion of Si, Na and K, and increased Al and Fe concentrations for subsequent smectite precipitation under alkaline conditions. Palygorskite developed by direct chemical precipitation from Mg-rich and relatively Al-poor solutions that were coeval with or post-dated dolomitization during downward-directed early diagenesis and by transformation from smectite which is unstable in the presence of Mg supplied by basement ophiolitic and dolomitic units in the depositional environment. Therefore, the presence of a gradational contact between smectitic claystone, altered tuff and tuff, and between palygorskite-bearing dolomite and claystone, and the link between smectite flakes, feldspar and palygorskite fibers with dolomite, as well as the presence of a transition between smectite and palygorskite, reveal that *in situ* precipitation of smectite and palygorskite, or conversion of smectite to palygorskite, was controlled by lithology, Al and Fe concentrations, and Mg/Ca ratios, all under alkaline micro- and macro-physicochemical environmental conditions.

ACKNOWLEDGMENTS

REFERENCES

Abdioğlu, E. and Arslan, M. (2005) Mineralogy, geochemistry and genesis of bentonites of the Ordo area, NE Turkey. *Clay Minerals*, **40**, 131−151.

Akbulut, A. and Kadir, S. (2003) The geology and origin of sepiolite, palygorskite and saponite in Neogene lacustrine sediments of the Serinhisar-Acıpayam basin, Denizli, SW Turkey. *Clays and Clay Minerals*, **51**, 279−292.

Altaner, S.P. and Grim, R.E. (1990) Mineralogy, chemistry, and diagenesis of tuffs in the Sucker Creek Formation (Miocene), Eastern Oregon. *Clays and Clay Minerals*, **38**, 561−572.

Baker, J.C. and Golding, S.D. (1992) Occurrence and palaeohydrological significance of authigenic kaolinite in the Aldebaran sandstone, Denison Trough, Queensland, Australia. *Clays and Clay Minerals*, **40**, 273−279.

Barnard, P.C. and Cooper, B.S. (1981) Oils and source rocks of the North Sea area. Pp. 169−175 in: *Petroleum Geology of the Continental Shelf of North West Europe* (L.V. IIIing and G.D. Hobson, editors). Heyden & Son, London.

Braiser, M.D. (1985) *Microfossils*. George Allen & Unwin, London, 193 pp.

Brindley, G.W. (1980) Quantitative X-ray analysis of clays. Pp. 411−438 in: *Crystal Structures of Clay Minerals and their X-ray Identification* (G.W. Brindley and G. Brown, editors). Monograph **5**, Mineralogical Society, London.

Çelik, M., Temel, A., Orhan, H. and Tunoğlu, C. (1997) Economic importance of clay and aluminium sulphate occurrences in west-southwest of Konya, Turkey. *Turkish Journal of Earth Sciences*, **6**, 85−94.

Christidis, G.E. (1998) Comparative study of the mobility of major and trace elements during alteration of an andesite and a rhyolite to bentonite in the islands of Milos and Kimolos, Aegean, Greece. *Clays and Clay Minerals*, **46,** 379−399.

Christidis, G. and Dunham, A.C. (1997) Compositional variations in smectites. Part II: Alteration of acidic precursors, a case study from Milos Island, Greece. *Clay Minerals*, **32**, 253−270.

Christidis, G. and Scott, P.W. (1997) The origin and control of colour of white bentonites from the Aegean islands of Milos and Kimolos, Greece. *Mineralium Deposita*, **32**, 271−279.

Christidis, G., Scott, P.W. and Marcopoulast, T. (1995) Origin of the bentonite deposits of Eastern Milos and Kimalos, Greece: geological, mineralogical and geochemical evidence. *Clays and Clay Minerals*, **43**, 63−77.

Clayton, R.N. and Mayeda, T. (1963) The use of bromine pentafluoide in the extraction of oxygen from oxides and silicates for isotopic analysis. *Geochimica et Cosmochimica Acta*, **27**, 47−52.

Colson, J., Cojan, I. and Thiry, M. (1998) A hydrological model for palygorskite formation in the Danian continental

facies of the Provence Basin (France). *Clay Minerals*, **33**, 333−347.

Compton, J.S. (1991) Origin and diagenesis of clay minerals in the Monterey Formation, Santa Maria Basin Area, California. *Clays and Clay Minerals*, **39**, 449−466.

Craig, H. (1961) Isotopic variations in meteoric waters. *Science*, **133**, 1702−1703.

Ece, Ö.İ. and Çoban, F. (1994) Geology, occurrence and genesis of Eskişehir sepiolites, Turkey. *Clays and Clay Minerals*, **42**, 81−92.

Galán, E. and Ferrero, A. (1982) Palygorskite-sepiolite clays of Lebrija, southern Spain. *Clays and Clay Minerals*, **30**, 191−199.

Grim, R.E. and Güven, N. (1978) *Bentonites, Geology, Mineralogy, Properties and Uses*. Elsevier, Amsterdam, pp. 13−137.

Güven, N. (1988) Smectites. Pp. 497−559 in: *Hydrous Phyllosilicates* (S.W. Bailey, editor). Reviews in Mineralogy **19**, Mineralogical Society of America, Washington, D.C.

Hynes, A. (1980) Carbonatization and mobility of Ti, Y, and Zr in Ascot Formation metabasalts, SE Quebec. *Contributions to Mineralogy and Petrology*, **75**, 79−87.

Iijima, A. and Tada, R. (1981) Silica diagenesis of Neogene diatomaceous and volcaniclastic sediments in northern Japan. *Sedimentolgy*, **28**, 185−200.

Inglès, M. and Anadón, P. (1991) Relationship of clay minerals to depositional environment in the non-marine Eocene Pontils Group, SE Ebro basin (Spain). *Journal of Sedimentary Petrology*, **61**, 926−939.

James, N.P. (1972) Holocene and Pleistocene calcareous crust (caliche) profiles: creteria for subaerial exposure. *Journal of Sedimentary Petrology*, **42**, 817−836.

Jamoussi, F., Ben Aboud, A. and López-Galindo, A. (2003) Palygorskite genesis through silicate transformation in Tunisian continental Eocene deposits. *Clays Minerals*, **38**, 187−199.

Jones, J.B. and Segnit, E.R. (1971) The nature of opal I. Nomenclature and constituent phases. *Journal of Geological Society of Australia*, **18**, 57−68.

Kadir, S. and Karakaş, Z. (2002) Mineralogy, chemistry and origin of halloysite, kaolinite and smectite from Miocene ignimbrites, Konya, Turkey. *Neues Jahrbuch für Mineralogie, Abhandlungen*, **177**, 113−132.

Karakaş, Z. and Kadir, S. (1998) Mineralogical and genetic relationships between carbonate and sepiolite-palygorskite formations in the Neogene lacustrine Konya Basin, Turkey. *Carbonates and Evaporites*, **13**, 198−206.

Keller, J., Jung, D., Burgath, K. and Wolff, F. (1977) Geologie und petrographie des Neogenen Kalkalkali-Vulkanismus von Konya (Erenler Dağ-Alaca Dağ-massiv, Zentral-Anatolien). *Geologisches Jahrbuch Hessen*, **25**, 37−117.

Knox, G.J. (1977) Caliche profile formation. Saldanha Bay (South Africa). *Sedimentology*, **24**, 657−674.

Kunze, G.W. and Dixon, J.B. (1986) Pretreatment for mineralogical analysis. Pp. 91−99 in: *Methods of Soil Analysis, Part I, Physical and Mineralogical Methods* 2nd edition (A. Klute, editor). Soil Science Society of America, Madison, Wisconsin.

Lawrence, J.R. and Taylor, H.R. (1971) Deuterium and oxygen-18 correlation: Clay minerals and hydroxides in Quaternary soils compaired to meteoric water. *Geochimica et Cosmochimica Acta*, **35**, 993−1003.

Lawrence, J.R. and Taylor, H.R. (1972) Hydrogen and oxygen isotope systematics in weathering profiles. *Geochimica et Cosmochimica Acta*, **36**, 1377−1393.

MacLean, W.H. and Kranidiotis, P. (1987) Immobile elements as monitors of mass transfer in hydrothermal alteration: Phelps Dodge massive sulfide deposits, Matagami, Quebec. *Economic Geology*, **2**, 951−962.

Moore, D.M. and Reynolds, R.C. (1989) *X-ray Diffraction and the Identification and Analysis of Clay Minerals*. Oxford University Press, Oxford, 332 pp.

Mount, J.F. and Cohen, A.S. (1984) Petrology and geochemistry of rhizoliths from plio-Pleistocene fluvial and marginal lacustrine deposits, East Lake Turkana, Kenya. *Journal of Sedimentary Petrology*, **54**, 263−275.

Murphy, J.B. and Hynes, A.J. (1986) Contrasting secondary mobility of Ti, P, Zr, Nb, and Y in two metabasaltic suites in the Appalachians. *Canadian Journal of Earth Sciences*, **23**, 1138−1144.

Müller, G., Irion, G. and Förstner, U. (1972) Formation and diagenesis of inorganic Ca-Mg carbonates in the lacustrine environment. *Naturwissenschaften*, **59**, 158−164.

Özgüner, A.M., Büyüktemiz, M., Kılıç, M.F. and Demirci, A.R. (1987) Konya yöresi seramik hammaddeleri etüdü, 2 cilt. MTA Report No. 8371. (Unpublished).

Rodas, M., Luque, F.J., Mas, R. and Garzon, M.G. (1994) Calcretes, palycretes and silcretes in the paleogene detrital sediments of the Dueo and Tajo Basins, central Spain. *Clay Minerals*, **29**, 273−285.

Savin, S.M. and Epstein, S. (1970) The oxygen and hydrogen isotope geochemistry of clay minerals. *Geochimica et Cosmochimica Acta*, **34**, 25−42.

Şenel, M. (2002) 1/500.000 scale geological map of Turkey − Konya, General Directorate of Mineral Research and Exploration of Turkey.

Sheppard, S.M.F. (1986) Characterization and isotopic variations in natural waters. Pp. 141−162 in: *Stable Isotopes in High Temperature Geological Processes* (J.W. Valley, H.P. Taylor and J.R. O'Neil, editors). Reviews in Mineralogy **16**, Mineralogical Society of America, Washington, D.C.

Sheppard, S.M.F. and Gilg, H.A. (1996) Stable isotope geochemisty of clay minerals. *Clay Minerals*, **31**, 1−24.

Singer, A. (1979) Palygorskite in sediments: detrital, diagenetic, or neoformed − a critical review. *Geologische Rundschau*, **68**, 996−1008.

Singer, A. (1989) Palygorskite and sepiolite group minerals. Pp. 829−872 in: *Minerals in Soil Environments* (J. B. Dixon and S. B. Weed, editors). Soil Science Society of America, Madison, Wisconsin, USA.

Stamatakis, M.G., Hein, J.R. and Magganas, A.C. (1989) Geochemistry and diagenesis of Miocene lacustrine siliceous sedimentary and pyroclastic rocks, Mytilinii basin, Greece. *Sedimentary Geology*, **64**, 65−78.

Suludere, Y., Aydoğan, N., Özgüner, A.M. and Atilla, A. (1986) *Toçak yaylası (Konya − Beyşehir − Damlapınar) kaolen sahası. Dülger Kışlağı (Konya − Seydişehir − Çavuş) ve Helaloğlu yaylası (Konya − Beyşehir − Doğanbey) bentonit sahaları maden jeolojisi raporu*. MTA Report No 8071 (unpublished)

Taylor, H.P. (1974) The application of oxygen and hydrogen isotope studies to problems of hydrothermal alteration and ore deposition. *Economic Geology*, **69**, 843−883.

Taylor, H.P. (1979) Oxygen and hydrogen relationships in hydrothermal mineral deposits. Pp. 236−277 in: *Geochemistry of Hydrothermal Ore Deposits*, 2nd edition (H.L. Barnes, editor). Wiley, New York.

Teale, C.T. and Spears, D.A. (1986) The mineralogy and origin of some Silurian bentonites, Welsh Borderland, UK. *Sedimentology*, **33**, 757−765.

Temel, A., Çelik, M. and Tunoğlu, C. (1995) Konya Batı-Güneybatısında yeralan Neojen yaşlı volkanosedimater basenindeki kil oluşmları. *VII National Clay Symposium, Ankara*, pp. 32−45.

Temel, A., Gündoğdu, N.M. and Gourgaud, A. (1998) Petrological and geochemical characteristics of Cenozoic high-K calc-alkaline volcanism in Konya, central Anatolia,

Turkey. *Journal of Volcanology and Geothermal Research*, **85**, 447−471.

Torres-Ruiz, J., López-Galindo, A., González-López and Delgado, A. (1994) Geochemistry of Spanish sepiolite-palygorskite deposits: Genetic considerations based on trace elements and isotopes. *Chemical Geology*, **112**, 221−245.

Tucker, M.E. and Bathurst, R.G.C. (1990) *Carbonate Diagenesis*. Blackwell Scientific Publications, **1**, Oxford, UK, 312 pp.

Umut, M., Karabıyıkoğlu , M., Saraç, G., Bulut, V., Demirci, A.R., Erkan, M., Kurt, Z., Metin, S. and Özgönül, E. (1987) *Tuzlukçu − Ilgın − Doğanhisar − Doğanbey Konya ili ve dolayının jeolojisi*. MTA Report No. 8246, 38 p. (Unpublished)

Velde, B. (1995) *Origin and Mineralogy of Clays. Clays and the Environment*. Springer, France, 334 pp.

Weaver, C.E. (1989) *Clays, Muds, and Shales*. Developments in Sedimentology, 44, Elsevier, Amsterdam, 819 pp.

Weaver, C.E. and Beck, K. (1977) Miocene of the S.E. United States: A Model for chemical sedimentation in a peri-marine environment. Special Issue. *Sedimentary Geology*, **17**, 1−234.

Winchester, J.A. and Floyd, P.A. (1977) Geochemical discrimination of different magma series and their differentiation products using immobile elements. *Chemical Geology*, **20**, 245−252.

Wright, V.P. (1984) The significance of needle-like calcite in a Lower Carboniferous paleosol. *Geological Journal*, **19**, 23−32.

Wright, V.P. and Tucker, M.E. (1991) *Calcretes*. The International Association of Sedimentologists, Oxford, London, 352 pp.

Yalçın, H. and Gümüşer, G. (2000) Mineralogical and geochemical characteristics of Late Cretaceous bentonite deposits of the Kelkit Valley Region, Northern Turkey. *Clay Minerals*, **35**, 807−825.

Yui, T.F. and Chang, S.S. (1999) Formation conditions of vesicle/fissure-filling smectites in Penghu basalts: a stable-isotope assessment. *Clay Minerals*, **34**, 381−393.

Zedef, V., Öncel, M.S., Arslan, M., Döyen, A. and Söğüt, A.R. (1994) Alpin tipi kromit yataklarına jeokimyasal açıdan farklı bir örnek: Yeşildağ (Beyşehir-Konya) kromit yatağı. *S.Ü. Mühendislik-Mimarlık Fakültesi Dergisi*, **9**, 28−35.

Zielinski, R.A. (1982) The mobility of uranium and other elements during alteration of rhyolite ash to montmorillonite: A case study in the Troublesome formation, Colorado, USA. *Chemical Geology*, **35**, 185−204.